Developmental Cell
Short Article

PRC2 Controls *Drosophila* Oocyte Cell Fate by Repressing Cell Cycle Genes

Nicola Iovino,[1] Filippo Ciabrelli,[1] and Giacomo Cavalli[1,*]
[1]Institut de Génétique Humaine, CNRS, 141 rue de la Cardonille, Montpellier 34396, France
*Correspondence: giacomo.cavalli@igh.cnrs.fr
http://dx.doi.org/10.1016/j.devcel.2013.06.021

SUMMARY

The oocyte is a unique cell type that undergoes extensive chromosome changes on its way to fertilization, but the chromatin determinants of its fate are unknown. Here, we show that Polycomb group (PcG) proteins of the Polycomb repressive complex 2 (PRC2) determine the fate of the oocyte in *Drosophila*. Mutation of the enzymatic PRC2 subunit Enhancer of zeste (E(z)) in the germline abolishes spatial and temporal control of the cell cycle and induces sterility via transdetermination of the oocyte into a nurse-like cell. This fate switch depends on loss of silencing of two PRC2 target genes, *Cyclin E* and the cyclin-dependent kinase inhibitor *dacapo*. By contrast, the PRC1 component *Polycomb* (*Pc*) plays no role in this process. Our results demonstrate that PRC2 plays an exquisite role in the determination of the oocyte fate by preventing its switching into an endoreplicative program.

INTRODUCTION

In sexually reproducing organisms, propagation of the species relies on germ cells that produce gametes. Germ cells are specialized cells that undergo mitosis and meiosis during their life cycle (Sassone-Corsi and Fuller, 2011) and face several fate decisions during development. Starting from the tip of the *germarium* of the *Drosophila* ovary, germ cells undergo several fate choices that ultimately result in a stage 3 egg chamber containing a fully determined oocyte and 15 endocycling nurse cells (Figure 1A) (Spradling, 1993). Despite the great interest in understanding this process, the chromatin determinants that distinguish the oocyte from the nurse cells are unknown. PcG proteins are transcriptional repressors that regulate various developmental processes by silencing genes via posttranslational modification (PTM) of histones. PcGs are divided into two main complexes, named PRC1 and PRC2. PRC2 is highly conserved in invertebrates, vertebrates and plants, while the canonical PRC1 is not present in plants and nematodes (Whitcomb et al., 2007). Different variants of the PRC2 complex have been purified, and all of them have been shown to include the SET-domain-containing histone methyltransferase Enhancer of zeste (E(z)). E(z) methylates histone H3 on lysine 27 (H3K27me3), and it requires two other components for full catalytic activity: Suppressor of zeste 12 (Su(z)12) and Extra sex combs (Margueron and Reinberg, 2011). The PRC1 and PRC2 complexes functionally regulate homeotic genes, cell cycle genes, and the expression of imprinted genes, as well as cell proliferation, X chromosome inactivation, and primordial germ cell development (Ezhkova et al., 2009; Martinez and Cavalli, 2006; Sawarkar and Paro, 2010; Schwartz and Pirrotta, 2007; Yang et al., 2009; Yokobayashi et al., 2013). In addition, in *Drosophila* and *C. elegans*, PRC2 is required in the germline (Birve et al., 2001; Patel et al., 2012; Phillips and Shearn, 1990; Strome, 2005). In particular, a previous study showed that *E(z)* mutants can induce sterility (Phillips and Shearn, 1990). Here, we have investigated the mechanism by which E(z) protein controls oocyte cell fate determination and female fertility.

RESULTS AND DISCUSSION

PRC2-Specific Requirement for Oocyte Fate Determination

The function of E(z) in the *Drosophila* germline was analyzed by conducting an RNA interference (RNAi) knockdown (KD), by generating *E(z)* null mutant germline clones, and by using an *E(z)* temperature-sensitive (TS) allele. Nanos-Gal4 (nos-G4)-mediated E(z)-KD in the germline depleted E(z) protein from germline cells to undetectable levels (Figures 1B and 1C), while E(z) expression in follicle cells (FC) was unchanged (Ni et al., 2011). The KD caused complete sterility: oogenesis was arrested before the vitellogenic stages (Figure S1 available online; compare Figure S1A to Figure S1B and Figure S1C to Figure S1D), leading to the presence of degenerating stage 6 egg chambers in the ovary (see the yellow circle in Figure S1D). A similar phenotype was observed in *E(z)* null mutant germline clones (see the yellow circle in Figure S1G). To address whether other PRC2 components are required for ovary development, null mutant germline clones for *Su(z)12* were generated. Loss of *Su(z)12* function caused degeneration of the ovary prior to the vitellogenic stages (see the yellow circle in Figure S1I), which resulted in sterility, as reported elsewhere (Birve et al., 2001). Interestingly, E(z)-KD egg chambers did not contain an oocyte nucleus. Instead, 16 nurse-like cells were consistently detected (compare Movie S1 to Movie S2). In contrast, neither null mutant germline clones nor RNAi for *Pc*, a PRC1 member, showed sterility phenotypes or obvious defects in the oocyte (Figure S1K and Figure S1W). Together with previous reports (Gandille et al., 2010; Li et al., 2010) indicating that germline mutants for the other PRC1 components *polyhomeotic*, *Posterior sex combs*, and *Suppressor of zeste 2* do not present defects in the germline, these data suggested a specific, PRC1-independent requirement for PRC2 in oocyte development.

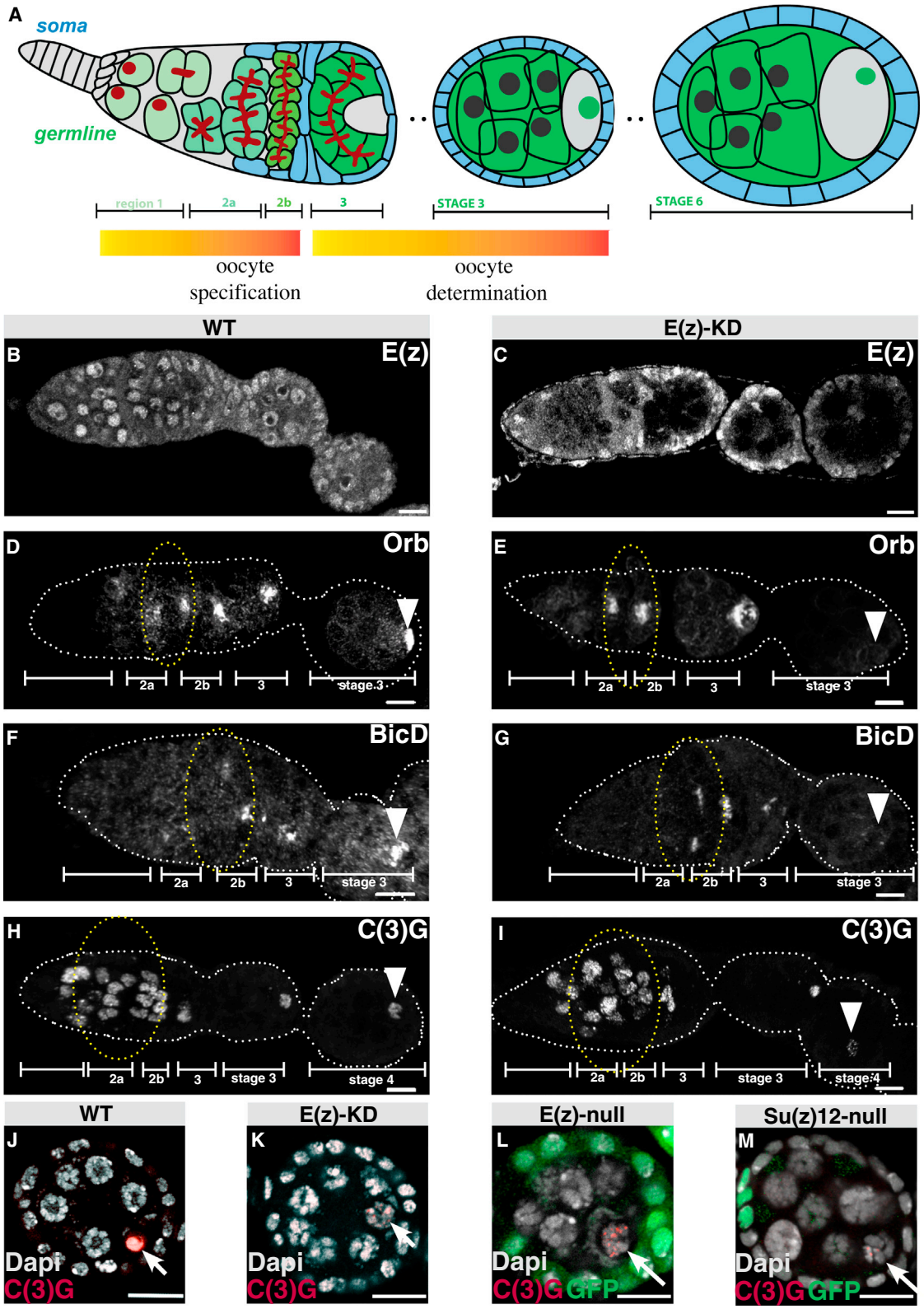

Figure 1. Depletion of E(z) Causes Sterility but Does Not Affect Oocyte Specification in Regions 2a and 2b

(A) A schematic diagram showing a cross-section of an ovariole from the *germarium* to stage 6. Germline is drawn in green, and somatic tissue is in blue.

(B) An ovariole up to stage 3 showing a uniform expression of E(z) in the germline and the FC.

(C) E(z)-KD ovariole up to stage 4 showing specific loss of E(z) staining in the germline and uniform expression in the FC.

(legend continued on next page)

PRC2 Is Required for Oocyte Determination, Not for Specification of the Preoocyte Fate

The next step was to determine when the oocyte switches fate following PRC2 inhibition. The oocyte is normally specified in the *germarium* from a syncytium of 16 germ cells. These cells are generated by four mitotic divisions of a single cystoblast (the offspring of a germ stem cell) with incomplete cytokinesis (Bate and Arias, 1993) (Figure 1A). The oocyte faces a major fate decision, since it has to exit the mitotic cycle and undergo meiosis to produce haploid gametes. In contrast to males, however, where all 16 cells will enter meiosis and become gametes, only one cell in *Drosophila* females will become the future oocyte, whereas the other 15 will enter an endocycle, becoming nurse cells and nurturing the oocyte until the late stages of oogenesis. Although PRC1 components were previously shown to control male germline differentiation (Chen et al., 2005), analysis of E(z)-KD in the male germline showed no obvious defects in the mitotic/meiotic switch or in male fertility (data not shown), suggesting that, in contrast to the female germline, PRC2 is dispensable in the male germline.

Oocyte determination involves two steps (Figure 1A). First, the future oocyte is specified in the *germarium* at regions 2a and 2b, concomitantly with the active transport of messenger RNAs (mRNAs) to the cell. Conditions disrupting active mRNA transport, such as those of *egalitarian* or *Bicaudal D* (*BicD*) mutants, or colchicine treatment, prevent the accumulation of specific oocyte markers and result in the generation of egg chambers containing 16 endocycling cells (Mach and Lehmann, 1997; Suter and Steward, 1991). In the second phase of oocyte determination, tight control of cell cycle genes and oocyte polarization genes drives the oocyte to its final transcriptionally silent and compacted karyosome fate by region 3 (Hong et al., 2003; Huynh et al., 2001; Lilly and Spradling, 1996; Mach and Lehmann, 1997; Mata et al., 2000). Specification of preoocytes at regions 2a and 2b can be traced by the localization of two specific markers (Lantz et al., 1994; Mach and Lehmann, 1997; Suter and Steward, 1991), Orb and BicD, around the nucleus, as well as by the assembly of a synaptonemal complex (SC) (Page et al., 2001) (compare ellipses in Figures 1D, 1F, and 1H to those in Figures 1E, 1G, and 1I, respectively). Whereas the initial distribution of preoocyte markers is correct in 90% of the E(z)-KD ovarioles (n = 50), preoocytes failed to become fully determined, as shown by the loss of Orb, BicD, and C(3)G by stages 3 and 4 (as observed in 80% of the egg chambers, n = 50) (arrowheads in Figures 1E, 1G, and 1I). At stage 4, E(z)-KD oocytes could still be identified by leftover SC C(3)G staining (arrow in Figure 1K). However, they did not present compact karyosomes and rather resembled nurse cells in size and shape, implying that they had undergone a similar number of endocycles (compare Figure 1J to Figure 1K; Figures S2A–S2H). Experiments using *E(z)* and *Su(z)12* germline null clones and an *E(z)* TS allele confirmed the proper specification of the oocyte (Figures S1M–S1V) and its failure to become fully determined in the absence of E(z) and Su(z)12 (Figures 1L and 1M and yellow circles in Figures S1O–S1T; for quantifications, see Experimental Procedures), thereby confirming the specificity of E(z)-KD, and confirming that polyploidy of the oocyte (arrow in Figures 1J–1M) is not a consequence of defects in the first step of oocyte specification. These data show that the oocyte switches into a nurse cell-like fate because of failure in the determination step of oocyte specification in the absence of PRC2.

PRC2 Acts by Direct Repression of the *CycE* and *dap* Genes

To understand the mechanism by which E(z) controls germline fate, the distribution of H3K27me3 and the expression of Su(z)12, another PRC2 component, were examined by immunofluorescence (IF). In early stage wild-type (WT) ovaries, H3K27me3 was present in all ovarian cells; however, by stage 4 of oogenesis, the H3K27me3 levels in nurse cells were markedly reduced (Figure 2A, arrowheads), although they remained unchanged in the FC and in the oocyte throughout oogenesis (Figures 2A, arrow, and 2G). In contrast, in E(z)-KD ovaries, H3K27me3 signals were strongly reduced in the germline but not in FC (Figures 2B and 2G; refer to Figure 1A to identify soma and germline). Consistent with a crucial role for E(z) in PRC2 integrity, Su(z)12 was also lost in the germline of E(z)-KD ovaries (compare Figures S2I and S2J to Figures S2K and S2L). In contrast to H3K27me3, the distribution of H3K27 acetylation (H3K27ac), which is catalyzed by a different enzyme (Tie et al., 2009), was present in all ovarian cells, and its distribution was not affected by E(z)-KD (Figures 2C and 2D). Consistent with the lack of phenotypic effects upon germline inactivation, Polycomb, an essential member of the PRC1 complex, was very weakly detected in

(D) WT ovariole from *germarium* to stage 3 (the contour of DAPI staining is indicated by white dots). Orb localizes in regions 2a and 2b (yellow ellipse) and posteriorly in stage 3 egg chamber (arrowhead).
(E) E(z)-KD ovariole from *germarium* to stage 4. Orb is properly localized in regions 2a and 2b (yellow ellipse) but fails to localize posteriorly in stage 3 and stage 4 egg chambers (arrowhead).
(F) WT ovariole from *germarium* to stage 3 showing proper BicD localization in regions 2a and 2b (yellow ellipse) and posteriorly in stage 3 egg chamber (arrowhead).
(G) E(z)-KD ovariole from *germarium* to stage 3 showing proper BicD localization in regions 2a and 2b (yellow ellipse) but mislocalization in stage 3 (arrowhead).
(H) WT ovariole from *germarium* to stage 4 showing the localization of the SC C(3)G in the *germarium* (yellow ellipse) and in stage 3 and stage 4 egg chambers (arrowhead).
(I) E(z)-KD ovariole from the *germarium* to stage 4, showing proper SC C(3)G localization in the *germarium* (yellow ellipse) but very weak or absent signal in stage 3 and stage 4 egg chambers (arrowhead).
(J) Stage 4 WT egg chamber showing a compact karyosome (arrow) identified by SC C(3)G staining.
(K) Stage 4 E(z)-KD egg chamber showing a nurse-cell like oocyte (arrow) identified by leftover SC C(3)G staining.
(L) Stage 4 null $E(z)^{731}$ clone (identified by the lack of green fluorescent protein [GFP] in the germline) showing a nurse-cell like oocyte (arrow) identified by leftover SC C(3)G staining.
(M) Stage 4 null $Su(z)12^{4}$ clone (identified by the lack of GFP in the germline) showing a nurse-cell like oocyte (arrow) identified by leftover SC C(3)G staining. Scale bar, 10 μm.
See also Figure S1.

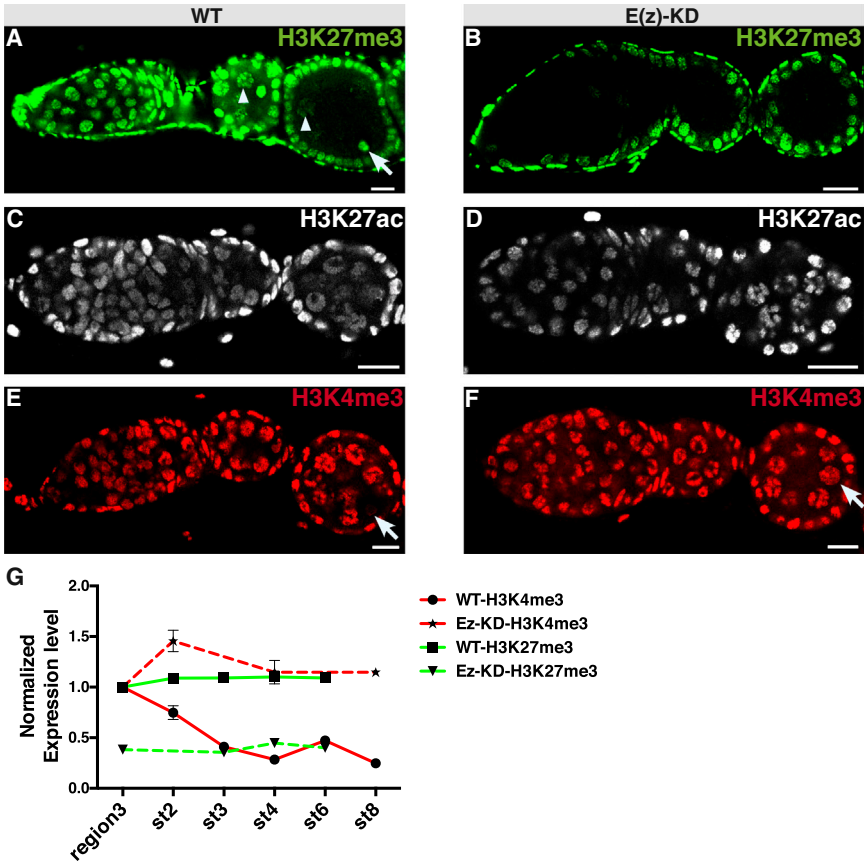

Figure 2. PRC2 and Associated PTM Dynamics in the Ovary

(A) WT ovariole up to stage 4 showing that H3K27me3, a PTM associated with E(z), is uniformly present in the FC and in the germline until stage 3 and drops in the nurse cells (arrowhead) by stage 4 but not in the oocyte (arrow).

(B) An E(z)-KD ovariole up to stage 4 showing specific loss of H3K27me3 staining in the germline and uniform expression in the FC.

(C) WT ovariole up to stage 3 showing a uniform expression of H3K27ac in the germline and the FC.

(D) An E(z)-KD ovariole up to stage 3 showing no mislocalization of H3K27ac.

(E) WT ovariole up to stage 4 showing that H3K4me3, a PTM associated with gene activation, is uniformly expressed in the FC and in the germline but not in the oocyte at stage 4 (arrow). The oocyte is identified by DAPI costaining (data not shown).

(F) An ovariole showing that ectopic H3K4me3 is present in the E(z)-KD oocyte at stage 4 (arrow). The oocyte is identified by C(3)G costaining (data not shown).

(G) Measured intensities from confocal sections relative to region 3 for H3K27me3 in green and H3K4me3 in red. The same intensities were measured in E(z)-KD ovaries (dashed lines). Error bars represent SEM. Scale bar, 10 μm.

See also Figure S2.

the germline (Figures S2M and S2N), and its distribution was unaffected by E(z)-KD (data not shown). Trimethylation of histone H3 on lysine 4 (H3K4me3), a PTM associated with genes that are being actively transcribed (Santos-Rosa et al., 2002), was also analyzed. In WT tissue, the H3K4me3 signal was present in all FC and nurse cells, but its abundance was reduced in the oocyte from stage 3 (Figures 2E and 2G), the developmental stage at which the oocyte nucleus is completely silenced and no transcription is detected. By contrast, H3K27ac and H3K4me1 were detected in the oocyte up until the late stages of development (Figures S2O and S2P), suggesting the possibility that enhancer regions may be bookmarked by histone modifications during oocyte maturation (Bonn et al., 2012; Kharchenko et al., 2011).

The transformed oocytes in E(z)-KD ovaries (identified by residual C(3)G staining) still retained H3K4me3 staining at stage 3 (arrow in Figures 2F and 2G), consistent with a fate switch from a transcriptionally silent karyosome to an active one. Indeed, the presence of H3K4me3 staining in the E(z)-KD oocyte is not simply a consequence of the loss of the H3K27me3 PTM because, in the E(z)-KD ovary, the levels of H3K4me3 in region 3 were not higher than those in the WT, even though H3K27me3 was absent (Figure 2G). Instead, these data suggest that, in contrast to the observations in WT oocytes, the levels of H3K4me3 do not decrease from stage 2 onward upon E(z)-KD.

In region 2b of the WT *germarium,* the cyst contains 16 cells that have exited the mitotic cycle, consistent with the loss of mitotic Cyclin A (CycA) and of phosphorylation of histone H3 on serine 10 (H3S10P). This is also consistent with the absence of 5-ethynyl-2′-deoxyuridine (EdU) incorporation, which is normally observed in S-phase cells (Figures 3A, 3C, 3M, 3N, and S3K). At this stage, the 16 cells face a new fate decision, since shortly afterward (region 3), 15 of them (the nurse cells) will enter the so-called endocycling phase and become polyploid, while the future oocyte reaches its fully determined state and progresses through meiosis. In E(z)-KD ovaries, ectopic S phases were observed in region 2b, as detected by EdU incorporation (Figures 3B and 3M) in the absence of mitotic markers (Figures 3D, 3N, and S3L), suggesting that these S-phase cells might be endocycling. The endocycles are driven by alternating pulses of the Cyclin E (CycE)/CdK2 complex and the kinase inhibitor Dacapo (Dap). Each nurse cell, in a cell autonomous manner, establishes a "flip-flop" mechanism, where pulses of CycE/CdK2 drive it into S phase, followed by pulses of Dap, which reset the cycle to G1 (de Nooij et al., 2000; Edgar and Orr-Weaver, 2001; Jones et al., 2000; Lilly and Spradling, 1996). Accordingly, CycE and Dap were detected in regions 1, 2a, and 3 of the *germarium* in WT ovaries but not in region 2b (Figures 3E, 3G, 3O, and 3P). Strikingly, however, ectopic expression of CycE and Dap was detected in region 2b upon E(z)-KD, in 90% (n = 25) and 80% (n = 37) of cases, respectively (Figures 3F, 3H, 3O, and 3P, and S3A–S3D, yellow ellipses). In order to ascertain whether the ectopic expression of CycE and Dap reflected transcriptional defects, we performed in situ hybridization against *CycE* and *dap* mRNA. Ectopic transcription of *CycE* and *dap* mRNA was detected in region 2b in

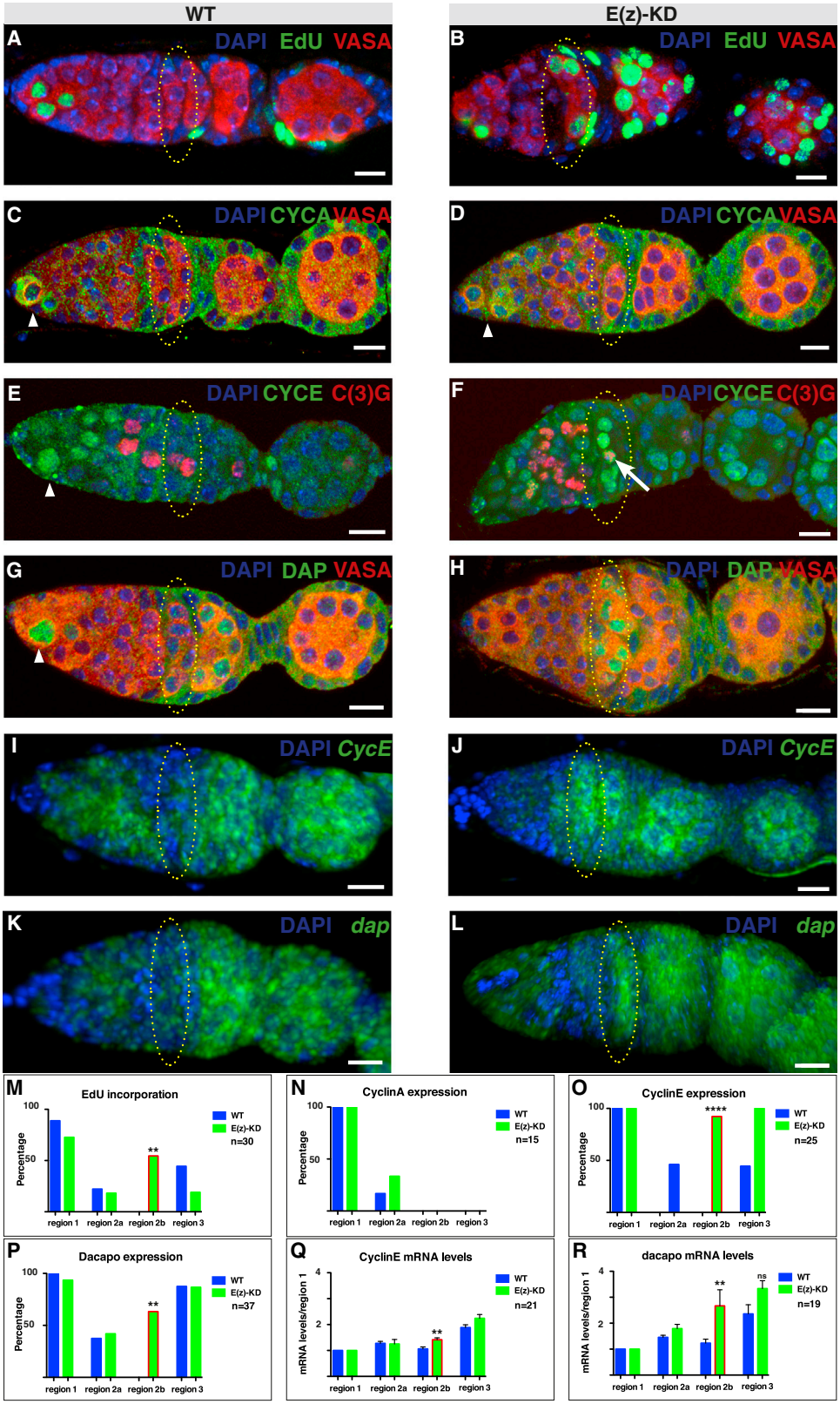

(legend on next page)

E(z)-KD *germarium* compared to WT (Figures 3I–3L, 3Q, and 3R). Region 2b cells were thus actively engaged in a proper endocycle, as also confirmed by the out-of-phase (flip-flop) expression of EdU (S phases) and Dap (Figures S3E–S3H). *E(z)* germline clones also showed Dap overexpression in *E(z)* null cells of region 2b (Figures S3I and S3J), confirming the results obtained with E(z)-KD.

An important question is whether *CycE* and *dap* are direct targets of E(z). To test this possibility, chromatin immunoprecipitation (ChIP) assays were performed using anti-E(z) and anti-H3K27me3 antibodies followed by quantitative real-time PCR (qPCR) along the genomic loci of *dap* and *CycE*, comparing WT with E(z)-KD ovaries. The results show that both the *dap* and *CycE* loci (Figures 4A–4D, S4A, and S4B) were enriched for E(z) and its H3K27me3 repressive mark. Importantly, this enrichment was specifically reduced in E(z)-KD ovaries (Figures 4A–4D, blue line; Figures S4A and S4B), showing that E(z) binding and deposition of H3K27me3 occur in germline cells.

Since PRC2 components regulate many genes during development, we next examined whether *dap* and *CycE* are the critical targets that must be repressed by PRC2 to maintain oocyte identity. Simultaneous overexpression of *CycE* and *dap* complementary DNAs (cDNAs) in a WT germline background pushed the oocyte toward a nurse-like polyploid cell fate (Figures 4E–4H) and resulted in sterility. Overexpression of either CycE or Dap alone was not sufficient (data not shown), showing that ectopic expression of both genes can switch the oocyte to the endocycle program, mimicking the E(z)-KD phenotype.

DISCUSSION

Together, our data show that PRC2 controls oogenesis by direct corepression of *CycE* and *dap* in a time window that stretches from region 2b to region 3. This prevents improper endocycling, before the oocyte becomes fully silenced and determined by stage 3. Interestingly, E(z) levels rapidly drop in the germline at stage 4, suggesting that the continuous presence of PRC2 is no longer required after oocyte determination. This observation is consistent with the fact that depletion of E(z) after stage 3 using a late Gal4 driver does not affect oocyte fate (Figures S4E and S4F).

Although differences between PRC1 and PRC2 have been previously reported in mammals (Lessard et al., 1999; Sauvageau and Sauvageau, 2010) and *Drosophila* (Richter et al., 2011), it is crucial to understand whether the molecular differences reflect specific biological roles for each of the two complexes. Here, PRC2 was shown to control oocyte cell fate determination, whereas PRC1 components, such as Pc, had no obvious function in the oocyte, consistent with absence of Pc from the germline (Figure S2M and S2N). Intriguingly, a different situation is seen in the fly male testis, where PRC1 components are required in the germline (Chen et al., 2011) while PRC2 is dispensable. Therefore, the production of gametes is a critical biological function that separates the function of these two complexes.

Although a few genes that are responsible for oocyte determination have been identified previously, none is known to act on chromatin. Our identification of PRC2 as a chromatin effector complex that is required to fix the oocyte fate offers the possibility of starting to dissect the molecular mechanisms that transduce the early asymmetry between the preoocyte and the surrounding cells into a terminally determined fate.

EXPERIMENTAL PROCEDURES

Genetics, Transgenes, and Fly Strains

Mitotic germline stem cell clones of loss-of-function mutants were generated using the Flippase/Flippase recombination target (FLP-FRT) technique. For clone generation, $E(z)^{731}$ FRT2A, $Su(z)12^{4}$ FRT2A (J. Mueller), and Pc^{XT109}

Figure 3. Depletion of E(z) Induces Ectopic DNA Replication in Region 2b

(A) WT *germarium* showing S phases labeled by EdU incorporation in region 1 but not in region 2b (yellow ellipse). The germline is labeled by Vasa antibody staining (red).

(B) E(z)-KD *germarium* showing S phases labeled by EdU incorporation in region 1 and in region 2b (yellow ellipse). Here, as well as in (A), the germline is labeled by Vasa antibody staining (red).

(C and D) WT *germarium* (C) and an E(z)-KD *germarium* (D) showing mitotic CycA in region 1 but not in region 2b (yellow ellipse). The germline is labeled by Vasa antibody staining (red).

(E) WT ovariole showing CycE in region 1 (arrowhead) of the *germarium* and stage 1 egg chamber but not in region 2b (yellow ellipse). The oocyte in region 2b is identified by synaptonemal complex C(3)G staining (red).

(F) E(z)-KD *germarium* showing mislocalization of CycE in region 2b (yellow ellipse). The oocyte in region 2b is identified by synaptonemal complex C(3)G staining (red), showing colocalization with CycE (arrow).

(G) WT ovariole showing proper localization of Dap in region 1 (arrowhead) of the *germarium* and region 3 but not in region 2b (yellow ellipse). The germline is labeled by Vasa antibody staining (red).

(H) E(z)-KD *germarium* showing mislocalization of Dap in region 2b (yellow ellipse). Here, as well as in (G), the germline is labeled by Vasa antibody staining (red).

(I) WT ovariole showing *CycE* mRNA localization in the *germarium* and stage 2 egg chamber. Note low/undetectable levels of *CycE* mRNA in region 2b (yellow ellipse).

(J) E(z)-KD ovariole showing *CycE* mRNA localization in the *germarium* and stage 2 egg chamber. Note misexpression of *CycE* mRNA in region 2b (yellow ellipse).

(K) WT ovariole showing *dap* mRNA localization in the *germarium* and stage 2 egg chamber. Note low/undetectable levels of *dap* mRNA in region 2b (yellow ellipse).

(L) E(z)-KD ovariole showing *dap* mRNA localization in the *germarium* and stage 2 egg chamber. Note misexpression of *dap* mRNA in region 2b (yellow ellipse).

(M) Fraction of WT and E(z)-KD *germaria* showing EdU incorporation for a given region. Note extra S phases in region 2b in E(z)-KD *germaria*.

(N) Fraction of WT and E(z)-KD *germaria* showing the correct CycA staining for a given region.

(O) Fraction of WT and E(z)-KD *germaria* showing CycE staining for a given region. Note CycE misexpression in region 2b in E(z)-KD *germaria*.

(P) Fraction of WT and E(z)-KD *germaria* showing Dap staining for a given region. Note Dap ectopic expression in region 2b in E(z)-KD *germaria*.

(Q) Intensities for *CycE* mRNA, measured from confocal sections of WT and E(z)-KD *germaria* relative to region 1. Note *CycE* mRNA misexpression in region 2b in E(z)-KD *germaria*.

(R) Intensities for *dap* mRNA, measured from confocal sections of WT and E(z)-KD *germaria* relative to region 1. Note *dap* mRNA misexpression in region 2b in E(z)-KD *germaria*. Error bars represent SEM. Statistical significance was calculated using an unpaired t test. $^{**}p < 0.005$; and $^{****}p < 0.0001$. Scale bar, 10 μm. See also Figure S3.

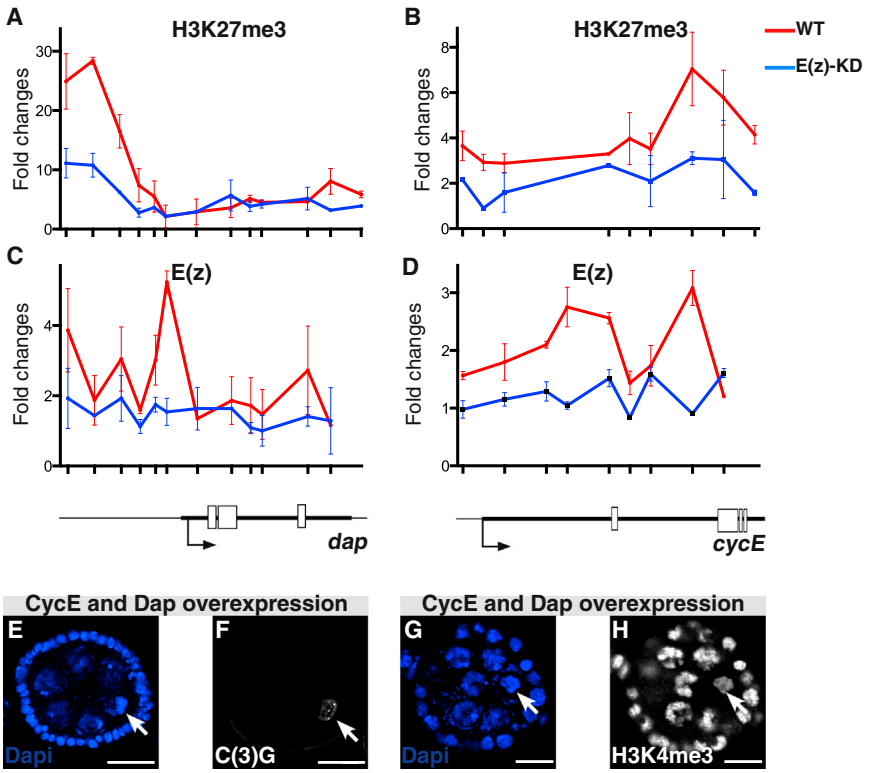

Figure 4. *Dap* and *CycE* Are Directly Bound and Repressed by E(z) to Control Oocyte Cell Fate

(A and B) Enrichment for H3K27me3 in WT (red) compared to the E(z)-KD (blue) determined by quantitative ChIP (qChIP) on *dap* and *CycE* genes. ChIP signals (represented as fold changes) were normalized to a negative control from the *PGRP-LE* gene. The genomic location of the *dap* and *CycE* genes are shown at the bottom.

(C and D) Binding of E(z) in WT (red) compared to the E(z)-KD (blue) determined by qChIP on *dap* and *CycE* genes. ChIP normalization and schematic annotations are as in (A) and (B).

(E) DAPI staining of a stage 4 egg chamber showing (arrow) the presence of a polyploid oocyte upon CycE and Dap overexpression.

(F) C(3)G staining of a stage 4 egg chamber showing (arrow) the reduction of C(3)G upon CycE and Dap overexpression.

(G) DAPI staining of a stage 4 egg chamber showing (arrow) the presence of a polyploid oocyte upon CycE and Dap overexpression.

(H) H3K4me3 staining of a stage 4 egg chamber showing (arrow) the persistence of H3K4me3 in the defective/endocycling oocyte upon CycE and Dap overexpression. The oocyte is identified by C(3)G costaining (data not shown). Error bars represent SEM.

See also Figure S4.

alleles were crossed with a hsFLP;Ubi-GFP FRT2A stock. An unmarked FRT2A stock was used as a WT control. Third instar larvae of the right genotype were heat shocked (37°C for 1 hr; heat shock performed on 3 consecutive days), and then adults were dissected 10 days after hatching (ah). Clones dissected later than 10 days ah accumulated stronger cell cycle defects, with polyploidy starting even before region 2b; therefore, we carefully dissected flies at 9 to 10 days ah. The oocyte polyploidy phenotype was quantified by counting stage 4 egg chambers from null clones (dissected from flies 10 days ah). Due to the stronger effect of the null alleles compared to KD, stage 4 egg chambers showed degeneration phenotype in 21% of the *E(z)* and 9% of the *Su(z)12* clones, compromising assessment of the oocyte polyploidy, and were therefore excluded from the quantification of polyploidy. Of the remaining *E(z)* and *Su(z)12* null clones, 32% and 23%, respectively, showed a polyploid oocyte while 6% and 13%, respectively, showed a partial polyploidy. Moreover, we observed also some defects in the early regions of the *germarium* in 12% of the *E(z)* null clones; 47 *E(z)* null clones and 28 *Su(z)12* null clones were examined. This indicates that null clones globally have a more severe phenotype (early degeneration) compared to KDs but that the dominant phenotype is still the transformation of the oocyte into a nurse-like fate. The following fly strains were used in the article: E(z) TRIP #33659 and Pc TRIP #33622. The following drivers were used for inducing RNAi in the germline: BL#25751 (Nos-Gal4) and Cog-Gal4 (drives Gal4 from stage 2/3 onward) (V. Barbosa). The flies of the right RNAi genotype were kept 3 to 4 days at 29°C along with WT flies and then dissected (25°C also gave similar phenotypes). The driver BL#31777 was used to overexpress CycE and Dap in the germline. The UASp-*Cyclin E* and UASp-*dacapo* constructs were created using a *Cyclin E* cDNA clone (C. Lehner), and *dacapo* cDNA clone was obtained from the Drosophila Genetic Resource Center (DGRC). The cDNAs were subcloned in a gateway cassette UASp promoter vector from DGRC and injected in fly embryos. Fly transformants with insertion on the second and third chromosomes, respectively, were recovered.

Histochemistry and Imaging

Antibody staining of ovaries was performed using our published protocols (Iovino et al., 2009). The following antibodies were used for whole-mount staining in this study: mouse anti-Orb, 1:1,000 (I. Busseau); mouse anti-BicD, 1:20 (B. Suter); mouse anti-C(3)G, 1:500 (I. Busseau); rabbit anti-H3K27me3, 1:100 (Millipore 07-449); mouse anti-H3K27ac, 1:100 (MABIO339); rabbit anti-H3K4me3, 1:100 (Millipore 07-473); mouse anti-CycA, 1:20 (Developmental Studies Hybridoma Bank), rabbit anti-CycE, 1:50 (H. McNeill); rabbit anti-CycE, 1:500 (Santa Cruz Biotechnology, sc-33748); mouse anti-Dap, 1:20 (Developmental Studies Hybridoma Bank); rabbit anti-Pc, 1:100; rabbit anti Su(z)12, 1:100 (J. Muller); rabbit anti-H3K4me1, 1:100 (Millipore 07-436); rabbit anti-H3S10P, 1:100 (Millipore 3H10). EdU incorporation was performed according to the manufacturer's guidelines (Click-iT EdU, Invitrogen). For E(z), we used two different antibodies. The first is a rabbit anti-E(z) (J. Muller) that was used at 1:100 dilution. The second was developed in our laboratory, and it is a rabbit antibody directed against the first 154 amino acids of the E(z) protein. Both antibodies gave the same results. All secondary antibodies were used at 1:1,000 dilution (Molecular Probes). RNA in situ hybridization procedures are described in Iovino et al. (2009). RNA sense and antisense probes were prepared from PCR products amplified using oligos ctacttggccgtcgac tacc and gccttctgggagatcactcg for *CycE* and oligos cccgagtcctgaatcctgtg and tttttggctgtctcttgcgc for *dap*.

Images were obtained with an inverted Zeiss LSM780 fitted with a UV laser. To quantify protein levels, we used Imaris for three-dimensional visualization of stacks of ~30 0.48-μm confocal sections of staged egg chambers. Nuclei were detected using DAPI staining and a threshold-based Isosurface segmentation. Average staining intensity in the segmented nuclei of interest was then measured.

ChIP

Same amounts of dissected ovaries from young WT (enriched in early stages) and E(z)-KD flies were dissected in PBS buffer. Ovaries were crosslinked in 1 ml A1 buffer (60 mM KCl, 15 mM NaCl, 15 mM HEPES [pH 7.6], 4 mM $MgCl_2$, 0.5% Triton X-100, 0.5 mM dithiothreitol (DTT), and complete EDTA-free protease inhibitor cocktail [Roche]), in the presence of 1.8% formaldehyde and homogenized at the same time in a douncer followed by incubation for 15 min at room temperature. Crosslinking was stopped by adding 225 mM glycine followed by incubation for 5 min. The homogenate was transferred

to a 1 ml tube and centrifuged for 5 min, 4,000 × g at 4°C. The supernatant was discarded, and the nuclear pellet was washed three times in 3 ml A1 buffer and once in 3 ml of A2 buffer (140 mM NaCl, 15 mM HEPES [pH 7.6], 1 mM EDTA, 0.5 mM EGTA, 1% Triton X-100, 0.5 mM DTT, 0.1% sodium deoxycholate, and protease inhibitors) at 4°C. After the washes, nuclei were resuspended in A2 buffer in the presence of 0.1% SDS and 0.5% N-lauroylsarcosine and incubated for 30 min on a rotating wheel at 4°C. Chromatin was sonicated using a Bioruptor (Diagenode) for 15 min (settings 30 s on, 30 s off, high power). Sheared chromatin had an average length of 300 to 700 base pairs. After sonication and 10 min high-speed centrifugation, fragmented chromatin was recovered in the supernatant. Chromatin was precleared by addition of 50 μl of Protein A-Agarose (PA) suspension (Roche 11134515001) followed by overnight incubation at 4°C. PA was removed by centrifugation, antibodies at dilution 1:100 were added to the supernatant (a control in the presence of rabbit preserum [Mock IP] was performed at the same time), and samples were incubated for 4 hr at 4°C in a rotating wheel. PA (50 μl) was added, and incubation was continued overnight at 4°C. Antibody-protein complexes were collected by centrifugation at 4,000 rpm for 1 min, and the supernatants were discarded. Samples were washed four times in A3 (A2+ 0.05% SDS) buffer and twice in 1 mM EDTA, 10 mM Tris (pH 8) buffer (each wash, 5 min at 4°C). Chromatin was eluted from PA in 250 μl of 10 mM EDTA, 1% SDS, 50 mM Tris (pH 8) at 65°C for 15 min, followed by centrifugation and recovery of the supernatant. The eluate was incubated overnight at 65°C to reverse crosslinks and treated with Proteinase K for 3 hr at 50°C. Sodium acetate (110 μM) was added to the samples, phenol-chloroform extracted, and ethanol precipitated in the presence of 20 μg glycogen. DNA was resuspended in 100 μl of water. Immunoprecipitated DNA was used to validate enrichment of specific DNA fragments by qPCR (see Figures S4A and S4B) Note that, for E(z) ChIP, the data presented were obtained with the antibody from Jürg Müller. The Cavalli antibody was also used in ChIP, with very similar results, but the IP quality was lower, as indicated by the larger fluctuation of the signals in the negative controls. Primer sequence lists are found in the Supplemental Experimental Procedures.

SUPPLEMENTAL INFORMATION

Supplemental Information includes Supplemental Experimental Procedures, four figures, and two movies and can be found with this article online at http://dx.doi.org/10.1016/j.devcel.2013.06.021.

ACKNOWLEDGMENTS

We thank Peter Follette, Tirtha Kamal Das, Jean-Réné Huynh, and Acaimo Gonzalez-Reyes for critically reading the manuscript. We thank Jürg Müller, Terry Orr-Weaver, Christian Lehner, Helena McNeill, Vitor Barbosa, and Isabelle Busseau for antibodies, reagents, and fly stocks. We thank Chloé Fallet for developing the rabbit anti-E(z) antibody in our laboratory. All the images were acquired and analyzed using the Montpellier RIO Imaging facility. Research at the G.C. laboratory was supported by grants from the European Research Council (ERC-2008-AdG no. 232947), the CNRS, the European Network of Excellence EpiGeneSys, the Agence Nationale de la Recherche, and the Association pour la Recherche sur le Cancer. N.I. was supported by a Long-Term European Molecular Biology Organization fellowship and by a fellowship from the Human Frontier Science Program Organization.

Received: January 22, 2013
Revised: June 3, 2013
Accepted: June 19, 2013
Published: August 8, 2013

REFERENCES

Bate, M., and Arias, A.M. (1993). The Development of *Drosophila melanogaster* (Cold Spring Harbor, NY: Cold Spring Harbor Laboratory Press).

Birve, A., Sengupta, A.K., Beuchle, D., Larsson, J., Kennison, J.A., Rasmuson-Lestander, A., and Müller, J. (2001). Su(z)12, a novel Drosophila Polycomb group gene that is conserved in vertebrates and plants. Development *128*, 3371–3379.

Bonn, S., Zinzen, R.P., Girardot, C., Gustafson, E.H., Perez-Gonzalez, A., Delhomme, N., Ghavi-Helm, Y., Wilczyński, B., Riddell, A., and Furlong, E.E. (2012). Tissue-specific analysis of chromatin state identifies temporal signatures of enhancer activity during embryonic development. Nat. Genet. *44*, 148–156.

Chen, X., Hiller, M., Sancak, Y., and Fuller, M.T. (2005). Tissue-specific TAFs counteract Polycomb to turn on terminal differentiation. Science *310*, 869–872.

Chen, X., Lu, C., Prado, J.R., Eun, S.H., and Fuller, M.T. (2011). Sequential changes at differentiation gene promoters as they become active in a stem cell lineage. Development *138*, 2441–2450.

de Nooij, J.C., Graber, K.H., and Hariharan, I.K. (2000). Expression of the cyclin-dependent kinase inhibitor Dacapo is regulated by cyclin E. Mech. Dev. *97*, 73–83.

Edgar, B.A., and Orr-Weaver, T.L. (2001). Endoreplication cell cycles: more for less. Cell *105*, 297–306.

Ezhkova, E., Pasolli, H.A., Parker, J.S., Stokes, N., Su, I.H., Hannon, G., Tarakhovsky, A., and Fuchs, E. (2009). Ezh2 orchestrates gene expression for the stepwise differentiation of tissue-specific stem cells. Cell *136*, 1122–1135.

Gandille, P., Narbonne-Reveau, K., Boissonneau, E., Randsholt, N., Busson, D., and Pret, A.M. (2010). Mutations in the polycomb group gene polyhomeotic lead to epithelial instability in both the ovary and wing imaginal disc in Drosophila. PLoS ONE *5*, e13946.

Hong, A., Lee-Kong, S., Iida, T., Sugimura, I., and Lilly, M.A. (2003). The p27cip/kip ortholog dacapo maintains the Drosophila oocyte in prophase of meiosis I. Development *130*, 1235–1242.

Huynh, J.R., Petronczki, M., Knoblich, J.A., and St Johnston, D. (2001). Bazooka and PAR-6 are required with PAR-1 for the maintenance of oocyte fate in Drosophila. Curr. Biol. *11*, 901–906.

Iovino, N., Pane, A., and Gaul, U. (2009). miR-184 has multiple roles in Drosophila female germline development. Dev. Cell *17*, 123–133.

Jones, L., Richardson, H., and Saint, R. (2000). Tissue-specific regulation of cyclin E transcription during Drosophila melanogaster embryogenesis. Development *127*, 4619–4630.

Kharchenko, P.V., Alekseyenko, A.A., Schwartz, Y.B., Minoda, A., Riddle, N.C., Ernst, J., Sabo, P.J., Larschan, E., Gorchakov, A.A., Gu, T., et al. (2011). Comprehensive analysis of the chromatin landscape in Drosophila melanogaster. Nature *471*, 480–485.

Lantz, V., Chang, J.S., Horabin, J.I., Bopp, D., and Schedl, P. (1994). The Drosophila orb RNA-binding protein is required for the formation of the egg chamber and establishment of polarity. Genes Dev. *8*, 598–613.

Lessard, J., Schumacher, A., Thorsteinsdottir, U., van Lohuizen, M., Magnuson, T., and Sauvageau, G. (1999). Functional antagonism of the Polycomb-Group genes eed and Bmi1 in hemopoietic cell proliferation. Genes Dev. *13*, 2691–2703.

Li, X., Han, Y., and Xi, R. (2010). Polycomb group genes Psc and Su(z)2 restrict follicle stem cell self-renewal and extrusion by controlling canonical and non-canonical Wnt signaling. Genes Dev. *24*, 933–946.

Lilly, M.A., and Spradling, A.C. (1996). The Drosophila endocycle is controlled by Cyclin E and lacks a checkpoint ensuring S-phase completion. Genes Dev. *10*, 2514–2526.

Mach, J.M., and Lehmann, R. (1997). An Egalitarian-BicaudalD complex is essential for oocyte specification and axis determination in Drosophila. Genes Dev. *11*, 423–435.

Margueron, R., and Reinberg, D. (2011). The Polycomb complex PRC2 and its mark in life. Nature *469*, 343–349.

Martinez, A.M., and Cavalli, G. (2006). The role of polycomb group proteins in cell cycle regulation during development. Cell Cycle *5*, 1189–1197.

Mata, J., Curado, S., Ephrussi, A., and Rørth, P. (2000). Tribbles coordinates mitosis and morphogenesis in Drosophila by regulating string/CDC25 proteolysis. Cell *101*, 511–522.

Ni, J.Q., Zhou, R., Czech, B., Liu, L.P., Holderbaum, L., Yang-Zhou, D., Shim, H.S., Tao, R., Handler, D., Karpowicz, P., et al. (2011). A genome-scale shRNA resource for transgenic RNAi in Drosophila. Nat. Methods *8*, 405–407.

Page, S.L., and Hawley, R.S. (2001). c(3)G encodes a Drosophila synaptonemal complex protein. Genes Dev. *15*, 3130–3143.

Patel, T., Tursun, B., Rahe, D.P., and Hobert, O. (2012). Removal of Polycomb repressive complex 2 makes C. elegans germ cells susceptible to direct conversion into specific somatic cell types. Cell Rep. *2*, 1178–1186.

Phillips, M.D., and Shearn, A. (1990). Mutations in polycombeotic, a Drosophila polycomb-group gene, cause a wide range of maternal and zygotic phenotypes. Genetics *125*, 91–101.

Richter, C., Oktaba, K., Steinmann, J., Müller, J., and Knoblich, J.A. (2011). The tumour suppressor L(3)mbt inhibits neuroepithelial proliferation and acts on insulator elements. Nat. Cell Biol. *13*, 1029–1039.

Santos-Rosa, H., Schneider, R., Bannister, A.J., Sherriff, J., Bernstein, B.E., Emre, N.C., Schreiber, S.L., Mellor, J., and Kouzarides, T. (2002). Active genes are tri-methylated at K4 of histone H3. Nature *419*, 407–411.

Sassone-Corsi, P., and Fuller, M.T. (2011). Germ Cells (Cold Spring Harbor, NY: Cold Spring Harbor Press).

Sauvageau, M., and Sauvageau, G. (2010). Polycomb group proteins: multi-faceted regulators of somatic stem cells and cancer. Cell Stem Cell *7*, 299–313.

Sawarkar, R., and Paro, R. (2010). Interpretation of developmental signaling at chromatin: the Polycomb perspective. Dev. Cell *19*, 651–661.

Schwartz, Y.B., and Pirrotta, V. (2007). Polycomb silencing mechanisms and the management of genomic programmes. Nat. Rev. Genet. *8*, 9–22.

Spradling, A.C. (1993). Developmental genetics of oogenesis. In The Development of *Drosophila melanogaster*, M. Bate and A. Martinez-Arias, eds. (Cold Spring Harbor, NY: Cold Spring Harbor Laboratory Press), pp. 1–70.

Strome, S. (2005, July 28). Specification of the germ line. WormBook, 1–10, http://dx.doi.org/10.1895/wormbook.1.9.1, http://www.wormbook.org.

Suter, B., and Steward, R. (1991). Requirement for phosphorylation and localization of the Bicaudal-D protein in Drosophila oocyte differentiation. Cell *67*, 917–926.

Tie, F., Banerjee, R., Stratton, C.A., Prasad-Sinha, J., Stepanik, V., Zlobin, A., Diaz, M.O., Scacheri, P.C., and Harte, P.J. (2009). CBP-mediated acetylation of histone H3 lysine 27 antagonizes Drosophila Polycomb silencing. Development *136*, 3131–3141.

Whitcomb, S.J., Basu, A., Allis, C.D., and Bernstein, E. (2007). Polycomb Group proteins: an evolutionary perspective. Trends Genet. *23*, 494–502.

Yang, X., Karuturi, R.K., Sun, F., Aau, M., Yu, K., Shao, R., Miller, L.D., Tan, P.B., and Yu, Q. (2009). CDKN1C (p57) is a direct target of EZH2 and suppressed by multiple epigenetic mechanisms in breast cancer cells. PLoS ONE *4*, e5011.

Yokobayashi, S., Liang, C.Y., Kohler, H., Nestorov, P., Liu, Z., Vidal, M., van Lohuizen, M., Roloff, T.C., and Peters, A.H. (2013). PRC1 coordinates timing of sexual differentiation of female primordial germ cells. Nature *495*, 236–240.